Sol−Gel Template Synthesis of Semiconductor Nanostructures

Brinda B. Lakshmi, Peter K. Dorhout, and Charles R. Martin*

Department of Chemistry, Colorado State University, Fort Collins, Colorado 80523

Received October 31, 1996. Revised Manuscript Received January 17, 1997[⊗]

The template method for preparing nanostructures entails synthesis of the desired material within the pores of a nanoporous membrane or other solid. A nanofibril or tubule of the desired material is obtained within each pore. Methods used previously to deposit materials within the pores of such membranes include electrochemical and electroless deposition and in situ polymerization. This paper describes the first use of sol−gel chemistry to prepare semiconductor nanofibrils and tubules within the pores of an alumina template membrane. TiO_2, WO_3, and ZnO nanostructures have been prepared. TiO_2 nanofibrils with diameters of 22 nm were found to be single crystals of anatase with the *c*-axis oriented along the fibril axis. Bundles of these fibrils were also found to be single crystalline, suggesting that the indiviual fibrils are arranged in a highly organized fashion within the bundle. Finally, 200 nm diameter TiO_2 fibrils were used as photocatalysts for the decomposition of salicylic acid.

Introduction

We have been exploring a general method for preparing nanomaterials that entails synthesis of the desired material within the pores of a nanoporous membrane.[1−3] The membranes used contain cylindrical pores with monodisperse diameters, and a nanoscopic fibril or tubule of the desired material is synthesized within each pore. This method has been used to make tubules and fibrils composed of polymers, metals, semiconductors, carbon, and Li ion intercalation materials.[1−3] Methods used to synthesize such materials within the pores of the template membranes include electroless metal deposition, electrochemical methods, and in situ polymerization.[1−3]

Sol−gel chemistry has recently evolved into a general and powerful approach for preparing inorganic materials.[4,5] This method typically entails hydrolysis of a solution of a precursor molecule to obtain first a suspension of colloidal particles (the sol) and then a gel composed of aggregated sol particles. The gel is then thermally treated to yield the desired material. It occurred to us that sol−gel chemistry could be done within the pores of the nanoporous template membranes to obtain tubules and fibrils of a variety of inorganic materials. We have recently used this combination of sol−gel and template methods to prepare fibrils and tubules of a variety of inorganic semiconducting materials including TiO_2, ZnO, and WO_3. We have found that single-crystal anatase-phase TiO_2 nanostructures can be obtained via this approach and that these nanostructures can be used as efficient photocatalysts. The results of these investigations are described here.

Experimental Section

Materials. Titanium isopropoxide, zinc acetate, $LiOH·H_2O$, WCl_6, 2,4-pentanedione, and salicylic acid (all from Aldrich), ethanol (McCormick Distilling Co.), and concentrated HCl (Mallinckrodt) were used as received. Purified water was obtained by passing house-distilled water through a Milli-Q (Millipore) water purification system. The alumina template membranes were either obtained commercially (Whatman Anopore filters, Fisher) or prepared in-house.[6,7] The commercial membranes had 200 nm diameter pores, and the in-house-prepared membranes had 22 nm diameter pores. The pore diameter of the in-house prepared membranes was obtained from a calibration curve of pore diameter vs voltage used during membrane synthesis.[7]

Synthetic Methods. TiO_2 tubules and fibrils were prepared using a sol−gel method similar to that described by Hamasaki et al.[8] Titanium isopropoxide (5 mL) was added to 25 mL of ethanol, and the resulting solution was stirred in an ice bath. To a second 25 mL portion of ethanol were added 0.5 mL of water and 0.5 mL of 0.1 M HCl. The titanium isopropoxide solution was removed from the ice bath and the ethanol/HCl/water solution was slowly added; unless otherwise noted, the temperature was maintained at 15 °C.

After ca. 60 s the resulting mixture turned milky white (sol formation). The alumina template membrane was immediately dipped into this solution for an immersion time that was varied between 5 and 60 s. After the desired immersion time, the membrane was removed from the sol and dried in air for 30 min at room temperature. The membranes were then placed in a tube furnace (in air), and the temperature was ramped (50 °C h^{-1}) to 400 °C. The membranes were heated at this temperature for 6 h, and the temperature was ramped back down (30 °C h^{-1}) to room temperature. A literature search produced one recent reference to the production of TiO_2 fibrils in membranes of this type; however, a much more difficult electrosynthetic method was used.[9]

ZnO fibers were prepared using a method similar to that of Sakhora et al.[10] To 20 mL of ethanol was added 0.35 g of zinc acetate, and the resulting mixture was boiled until a clear

* Corresponding author. E-mail: crmartin@lamar.colostate.edu.

⊗ Abstract published in *Advance ACS Abstracts,* February 15, 1997.

(1) Martin, C. R. *Science* **1994**, *266*, 1961.
(2) Martin, C. R. *Acc. Chem. Res.* **1995**, *28*, 61.
(3) Martin, C. R. *Chem. Mater.* **1996**, *8*, 1739.
(4) Brinker, C. J.; Scherer, G. W. *Sol−gel Science*; Academic Press, Inc.: New York, 1990. Hench, L. L.; West, J. K. *Chem. Rev. (Washington, D.C.)* **1990**, *90*, 33.
(5) O'Regan, B.; Moser, J.; Anderson, M.; Grätzel, M. *J. Phys. Chem.* **1990**, *94*, 8720; *Nature* **1991**, *335*, 737.
(6) Foss, C. A.; Tierney, M. J.; Martin, C. R. *J. Phys. Chem.* **1992**, *96*, 9001.
(7) Hornyak, G. L.; Martin, C. R. *J. Phys. Chem.*, submitted.
(8) Hamasaki, Y.; Ohkubo, S.; Murakami, K.; Sei, H.; Nogami, G. *J. Electrochem. Soc.* **1994**, *141*, 660.
(9) Hoyer, P. *Langmuir* **1996**, *12*, 1411.
(10) Sakhora, S.; Tickanen, L. D.; Anderson, M. A. *J. Phys. Chem.* **1992**, *96*, 11087.

S0897-4756(96)00557-1 CCC: $14.00

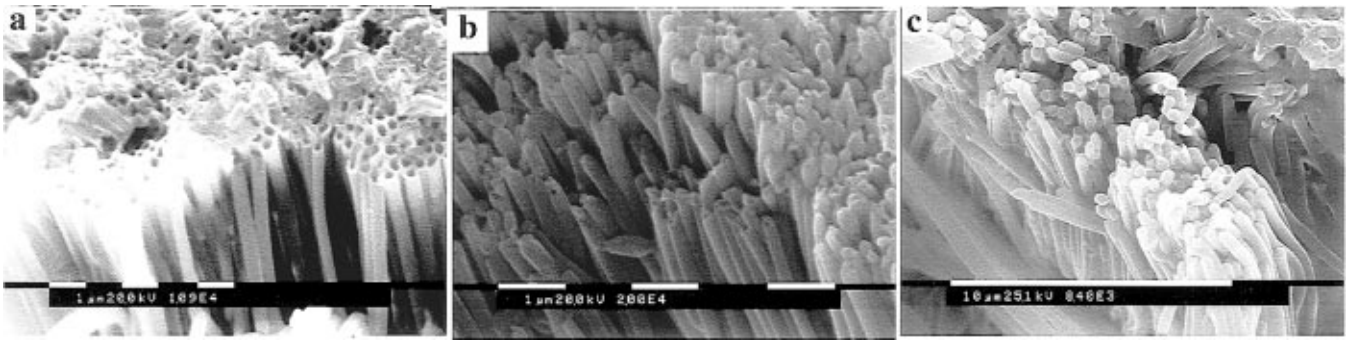

Figure 1. SEM images of TiO_2 tubules and fibrils prepared in the alumina membrane with 200 nm diameter pores. The sol was maintained at 15 °C, and the immersion time was varied from 5 to 60 s. (a) Immersion time = 5 s; remnants of the TiO_2 surface layer can be seen in this image. (b) Immersion time = 25 s. (c) Immersion time = 60 s.

solution was obtained (ca. 30 min). The volume was returned to 20 mL with ethanol, and 0.06 g of $LiOH \cdot H_2O$ was added. The resulting solution was ultrasonicated until a white suspension was obtained (ca. 1 h). The alumina membrane was immersed into this sol for 1 min, removed, and allowed to dry in air at room temperature for 30 min. The membrane was then heated in air at 120 °C for 6 h.

WO_3 fibers were prepared using a method similar to that of Nishide et al.[11] Ethanol (10 mL) was purged of air using an Ar bubbler, and 1 g of WCl_6 was added with continued Ar bubbling. 2,4-Pentanedione (2 mL) and H_2O (0.05 mL) were added, and the resulting mixture turned blue in color. The alumina membrane was immersed into this mixture for 1 min, removed and dried in air at room temperature for 30 min. The membrane was then placed in a furnace and the temperature was ramped (as before) to 550 °C. The membrane was heated at this temperature for 6 h, after which the temperature was ramped back down to room temperature.

These sol−gel synthetic methods yielded either tubules or fibrils of the desired semiconductor within the pores of the template membrane. In addition, thin films of the material were deposited on both faces of the membrane. One or both of these surface films were removed prior to analysis of the tubules or fibrils. This was accomplished by simply polishing the surface(s) of the membrane with sand paper (1500 grit).

Electron Microscopy. Scanning electron microscopic (SEM) images of the 200 nm diameter tubules and fibrils were obtained as follows: One surface layer was removed, and the membrane was glued (using Torr-Seal Epoxy, Varian) to a piece of paper towel. The membrane was glued with the polished face up. The resulting composite was immersed into 6 M aqueous NaOH for 10 min in order to dissolve the alumina. This yielded an ensemble of semiconductor tubules or fibrils that protruded from the epoxy surface like the bristles of a brush. This sample was attached to an SEM sample stub with silver paint (Spi), and 10 nm of Au−Pd was sputtered onto the surface using an Anatech sputter coater. The resulting sample was imaged using a Phillips 505 microscope.

Transmission electron microscopic (TEM) images of the semiconductor nanostructures were obtained as follows: Both surface layers were removed, and a piece of the resulting membrane was placed onto a carbon-film-coated TEM grid. The 6 M aqueous NaOH solution was then applied to the membrane in order to dissolve the alumina. The freed nanostructures adhered to the TEM grid and were imaged using a JEOL 2000 microscope. Electron diffraction data were also obtained using this instrument. The accelerating voltage of the electron beam was 100 kV and the camera length was 120 cm. A gold single crystal was used as a standard to check the camera length.

UV−Visible Spectroscopy. Both surface layers were removed, and the alumina membrane with the semiconductor nanostructures within the pores was placed in a custom-made sample holder. The sample holder was placed in the sample chamber of an Hitachi spectrophotometer. A simple absorption mode spectrum was obtained using a bare alumina membrane as the reference. Because the alumina template membranes are transparent throughout the visible and UV regions, these spectra showed the absorption band edge of the semiconductor nanostructures within the pores.

Photocatalysis. TiO_2 is known to be a good catalyst for photodecomposition of organic molecules.[12−19] The photocatalytic activity of the sol−gel-synthesized TiO_2 fibrils was evaluated using salicylic acid as the organic molecule to be decomposed. Samples in which the TiO_2 fibrils protruded from an epoxy surface were prepared as described for the SEM analyses. The area of epoxy surface used for these photocatalysis studies was 1 cm^2; this area contained ca. 10^9 200 nm diameter TiO_2 fibrils. After removal of the alumina template membrane in NaOH, the TiO_2 fibrils were rinsed in five portions of water to ensure complete removal of the NaOH. The fibrils were then immersed (overnight and in the dark) in 15 mL of 0.5 mM aqueous salicylic acid in order to allow organics present in the epoxy to leach out prior to the photocatalysis experiments.

The samples pretreated in this way were then immersed into a beaker containing 15 mL of fresh 0.5 mM aqueous salicylic acid. A quartz lid was placed over the top of the beaker, and the beaker was placed on the roof of the chemistry building in direct Colorado sunlight. Two controls were run at the same time and place as the fibrillar TiO_2 samples. The first consisted of an identical beaker with the same amount of salicylic acid solution; however, a thin film (200 nm thick) of TiO_2, prepared under identical conditions as the fibrillar sample, was used as the photocatalysts. The second control was also identical but contained no photocatalyst.

The concentration of salicylic acid in the three solutions was determined every 5 min for a total of 30 min. The salicylic acid concentration was determined from its characteristic UV absorbance (296 nm), using a calibration curve obtained from solutions of known concentration.

Results and Discussion

TiO_2 Tubules and Fibrils. Figure 1 shows SEM images of TiO_2 tubules and fibrils prepared in the alumina membrane with 200 nm diameter pores. Tubules were obtained if the membrane was immersed into the sol for a brief period (5 s, Figure 1a), whereas solid TiO_2 fibrils were obtained after long immersion times

(11) Nishide, T.; Yamaguchi, H.; Mizukami, F. *J. Mater. Sci.* **1995**, *30*, 4946.

(12) Fujishima, A.; Honda, K. *Nature* **1972**, *37*, 238.
(13) Matthew, R. W. *J. Phys. Chem.* **1987**, *91*, 3328.
(14) Kraeutler, B.; Bard, A. J. *J. Am. Chem. Soc.* **1978**, *100*, 5985.
(15) Ollis, D. F.; Hsiao, C.; Budiman, L.; Lee, C. *J. Catal.* **1984**, *88*, 89.
(16) Okamoto, K.; Yamamoto, Y.; Tanaka, H.; Tanaka, M.; Itaya, A. *Bull. Chem. Soc. Jpn.* **1985**, *58*, 2015.
(17) Mathews, R. W. *J. Catal.* **1987**, *97*, 565.
(18) Spanel, L.; Anderson, M. A. *J. Am. Chem. Soc.* **1991**, *113*, 2826.
(19) Goldstein, S.; Czapski, G.; Rabani, J. *J. Phys. Chem.* **1994**, *98*, 6586.

(60 s, Figure 1c). Intermediate immersion times yield tubules with very thick walls (25 s, Figure 1b). In all cases the tubules and fibrils were 50 μm long (the thickness of the template membrane) and had outside diameters of 200 nm (the diameter of the pores).

Whether tubules or fibrils are obtained is also determined by the temperature of the sol. The structures shown in Figure 1 were obtained by immersion of the alumina template membrane into a sol maintained at 15 °C. When the sol was 5 °C, thin-walled tubules were obtained even at long immersion times (1 min). In contrast, when the sol was maintained at 20 °C, solid TiO_2 fibrils were obtained even after very brief (5 s) immersion times. These results show that through control of temperature and immersion time, both tubules and fibrils can be prepared; in addition, the wall thickness of the tubules can be varied at will (e.g., Figure 1a,b).

The mechanism of formation of TiO_2 from acidified titanium alkoxide solutions is well documented.[20,21] In the early stages, sol particles held together by a network of −Ti−O− bonds are obtained. These particles ultimately coalesce to form a three-dimensional infinite network, the gel. That tubules are initially obtained when this process is done in the alumina membrane indicates that the sol particles adsorb to the pore walls. This is not surprising since the pore walls are negatively charged and the particles are positively charged.[22] An analogous situation occurs when positively charged electronically conductive polymers are synthesized within membranes containing anionic sites on their pore walls.[2]

In the conductive polymer case,[2] the rate of polymerization within the pore is faster than in bulk solution due to enhanced local concentration of oligomers adsorbed to the pore wall. A similar situation occurs in the sol−gel TiO_2 case. When a lower concentration of titanium isopropoxide (6 v/v % as opposed to the 20 v/v % used in Figure 1) was used to make the sol, gelation in bulk solution was extremely slow, even at room temperature. However, when the alumina membrane was dipped into this sol, solid fibrils of TiO_2 are obtained in the pores, even at short (5 s) immersion times. These results show that gelation occurs within the pores under conditions where gelation in bulk solution is negligibly slow. By analogy to the conductive polymer case[2] this is undoubtedly due to the enhancement in the local concentration of the sol particles due to adsorption on the pore wall.

Figure 2 shows an absorption spectrum for an alumina membrane containing 200 nm diameter TiO_2 fibrils within the pores. An abrupt increase in absorbance is observed at wavelengths below 389 nm. This corresponds to the bandgap of the TiO_2, and bulk samples of TiO_2 show an analogous absorption spectrum.[23] These fibrils (and even the 22 nm diameter fibrils to be discussed below) are too large in diameter to expect to see evidence for quantum confinement in the absorption spectrum.[23] However, preparing fibrils with diameters small enough to see evidence for quantum confinement is a goal of this research effort.

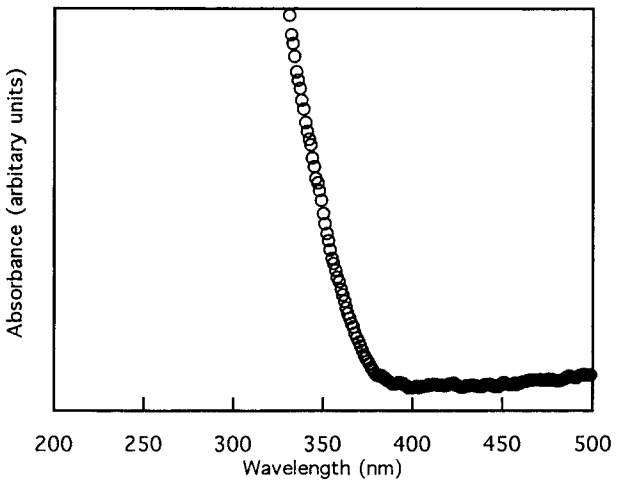

Figure 2. UV−visible spectrum of the 200 nm diameter TiO_2 fibrils.

Electron Diffraction Data for TiO_2 Fibrils Prepared in the Membrane with 22 nm Diameter Pores. Figure 3a shows a TEM image of the TiO_2 nanostructures obtained after dissolving away the 22 nm pore diameter membrane. Numerous images of this type were obtained, and in all cases bundles of the TiO_2 nanostructures were observed. The bundle sizes observed ranged from as small as 2−4 fibrils to as large as 10 or more fibrils. The main feature in Figure 3a that runs diagonally across the image consists of two bundles of fibrils, one on the right edge of the main feature and one on the left edge. In this case the bundles consist of approximately 3−4 fibrils. The electron diffraction data to be discussed below (Figure 3b) were obtained from a portion of the bundle on the left side of this main feature. A second set of two bundles is observed below this main feature; this second set of bundles also proceeds diagonally across the image but at a smaller angle.

Figure 3b shows the indexed electron diffraction pattern obtained from the center of the fibril bundle on the left side of the main feature in Figure 3a. The orientation of the images in Figure 3a,b is the same; that is, the **c*** axis in Figure 3b is parallel to the fibril bundle axis in Figure 3a. These data show that the fibrils are highly crystalline anatase-phase TiO_2, with the **c*** axis of the anatase oriented along the long axis of the fibril. Small fibril bundles throughout the sample displayed the same crystalline orientation; i.e., the reciprocal lattice direction [110] is almost always parallel to the electron beam, and the **c*** axis is along the fibril axis. We can conclude from these observations that the fibrils crystallize as long, prismatic crystals with the rare, and metastable, anatase mineralogical orientation [001] with {110}.[24]

Just as interesting, such small fibril bundles do not demonstrate a great deal of mosaic spread in the diffracted electron beam, as one would expect for polycrystalline materials or oriented polymer fiber samples.[25] Larger bundles of crystalline fibrils do show mosaic spreading of the reflections, but they remain oriented

(20) Lee, B. I.; Pope, E. J. A. *Chemical processing of ceramics*; Marcel Dekker, Inc.: New York, 1994.
(21) Livage, J.; Henry, M.; Sanchez, C. *Prog. Solid. State Chem.* **1988**, *18*, 259.
(22) Bischoff, B. L.; Anderson, M. A. *Chem. Mater.* **1995**, *7*, 1772.
(23) Enright, B.; Fitzmaurice, D. *J. Phys. Chem.* **1996**, *100*, 1027.
(24) Dana, J. D. (rewritten by Polache, C.; Berman, H.; Frondel, C.) *The system of mineralogy*; John Wiley: New York, 1955.
(25) Klug, H. P.; Alexander, L. E. *X-ray Diffraction procedures for polycrystalline and amorphous materials*; Wiley Interscience: New York, 1974.

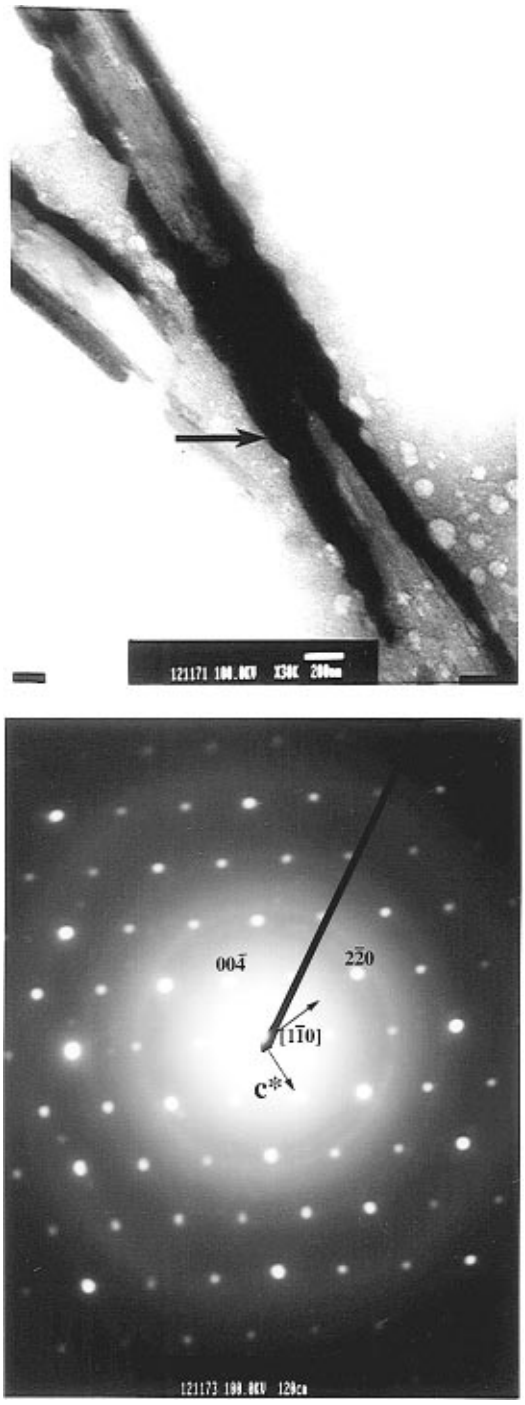

Figure 3. (a, top) TEM image of a bundle of 15 nm diameter TiO_2 fibrils. (b, bottom) Corresponding electron diffraction pattern.

along their [001] fiber axis. In addition, dark-field images of the fibril bundles indicate that the crystalline domains are very large. For example, bundles with diameters as large as 1 μm and lengths corresponding to the entire thickness of the template membrane (30 μm) are single crystals.

These data suggest that after the alumina template is removed, the individual fibrils are drawn together in an ordered fashion, like stacked 4 × 4 lumber. This stacking may be facilitated by vacant or labile ligand sites on the Ti atoms, which sit near the (110) faces (Figure 4). The Lewis acidic surface sites may be attracted to the oxide (or hydroxide) sites on other

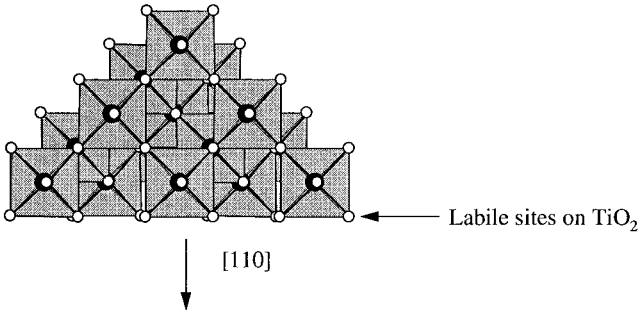

Figure 4. View down the *c*-axis of anatase showing the possible labile oxygen sites on the (110) face. TiO_6 polyhedra with filled circles (Ti) and open circles (O) are represented.

fibrils; these interactions could hold the fibrils in an oriented bundle that diffracts like a larger, single crystal (Figure 3b).

Highly oriented crystalline domains of other metastable phases have been shown to grow in an "internal" matrix, indicating that although our observations of oriented TiO_2 are unusual, they are not without precedent.[26] Furthermore, it is known that sol−gel syntheses can result in crystallization of metastable phases because of the lower temperatures often employed in such syntheses.[27] In addition, it has been previously shown that sol−gel synthesis can yield single-crystalline material, if the crystals are grown at very low temperatures.[28] Single-crystalline oriented MgO nanorods have also recently been reported, although this was not a sol−gel synthesis.[29] Oriented carbon nanofibers have been prepared by template synthesis.[30]

Finally, electron diffraction data from the 200 nm diameter TiO_2 fibrils show that these fibrils are also highly crystalline anatase. However, the data suggest that these larger-diameter fibrils are not single crystals.

Photocatalysis with the TiO_2 Fibrils. TiO_2 can be used as a photocatalyst to decompose organic molecules.[12−16] The mechanism is believed to involve absorption of a UV photon by TiO_2 to produce an electron−hole pair. These react with water to yield hydroxyl and superoxide radicals which oxidize the organic molecule. The ultimate products of these reactions are CO_2 and water.[18,19] Most investigations of the photocatalytic activity of TiO_2 have used UV lamps as the source and TiO_2 thin films or powders as the catalyst. We report here the use of sunlight as the source and immobilized template-synthesized TiO_2 fibrils as the catalyst.

Figure 5 shows a plot of salicylic acid concentration vs time of exposure of the solution to sunlight. The upper curve is for the solution that contained no TiO_2 photocatalyst. No loss of salicylic acid from the solution was observed. Indeed, there was a slight increase in concentration with time, due to evaporation of water; that evaporation occurred is proven by the appearance of water drops on the quartz lid. The lower curve in

(26) (a) Lin, J.; Cates, E.; Bianconi, P. A. *J. Am. Chem. Soc.* **1994**, *116*, 4738. (b) Bianconi, P. A.; Lin, J.; Strzelecki, A. *Nature* **1991**, *349*, 315.
(27) Lange, F. F. *Science* **1996**, *273*, 903.
(28) Spanhel, L.; Anderson, M. A. *J. Am. Chem. Soc.* **1991**, *113*, 2826.
(29) (a) Yang, P.; Leiber, C. M. *Science* **1996**, *273*, 1836. (b) Itoh, H.; Utamapanya, S.; Stark, J. V.; Klabunde, K. J.; Schlup, J. R. *Chem. Mater.* **1993**, *5*, 71.
(30) Kyotani, T.; Tsai, L.; Tomita, A. *Chem. Mater.* **1996**, *8*, 2109.

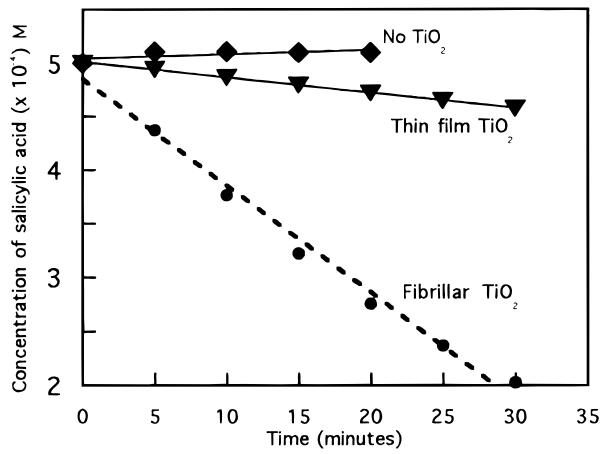

Figure 5. (a) Photodecomposition of salicylic acid in sunlight. Data for no photocatalyst, the thin-film TiO_2 photocatalyst, and the fibrillar (200 nm) TiO_2 photocatalyst are shown.

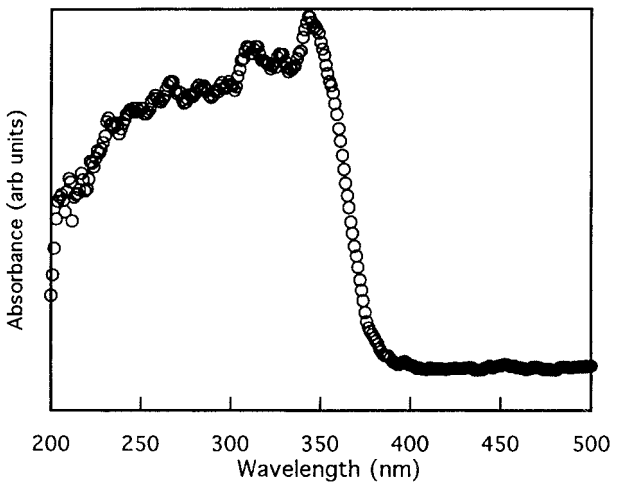

Figure 7. UV−visible spectrum of the 200 nm diameter ZnO fibrils.

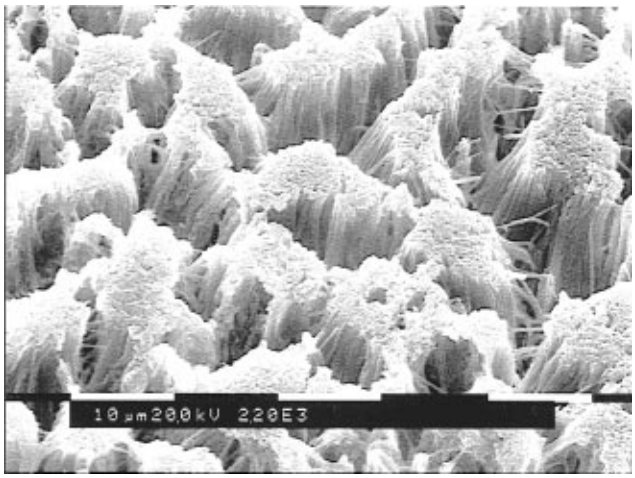

Figure 6. SEM image of 200 nm diameter ZnO fibrils.

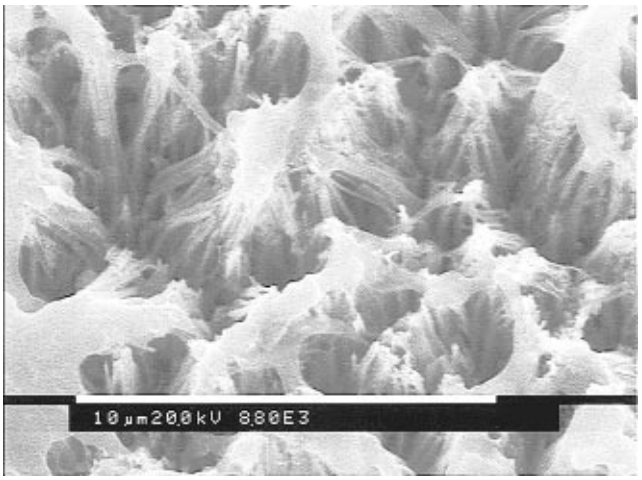

Figure 8. SEM image of 200 nm diameter WO_3 fibrils.

Figure 5 is for the solution that contained the fibrillar TiO_2 photocatalyst. A rapid (relative to the thin-film catalyst, middle curve) decrease in salicylic acid concentration was observed. Indeed, the rate of photodecomposition for the fibrillar catalyst is an order of magnitude higher than for the thin-film catalyst (see kinetic analysis below).

Both the thin film and fibrillar catalyst were supported on an epoxy surface with an area of 1 cm^2. The enhancement in rate for the fibrillar catalyst is due to the higher total surface area of TiO_2 exposed to solution. Indeed, if it is assumed that the surface area of the thin-film catalyst is 1 cm^2 and that all of the surfaces of the fibrils are catalytically active, an enhancement in rate of 315 would be predicted for the fibrillar catalyst. This calculated enhancement arises because the total calculated surface area of the fibrils is 315 cm^2 of TiO_2 surface area/cm^2 of substrate epoxy surface area. This corresponds to 5.1 m^2 of TiO_2 surface area/g of anatase fibrils. Even higher surface areas would be expected for tubules or smaller diameter fibrils.

That the experimental enhancement in rate is less is not surprising. First, the surface of the TiO_2 thin-film catalyst is undoubtedly not atomically smooth, meaning that its true catalytic surface area is greater than the assumed 1 cm^2. Second, SEM images show that the fibrils do not stand straight up but rather "lean" against each other to form clumps or bunches. As a result, large portions of the fibril surfaces are shaded from the sunlight. Hence, this prototype fibrillar catalyst is not optimal. Variables to be considered for optimization include diameter and aspect ratio of the fibrils (length divided by diameter) and distance between fibrils.

The data in Figure 5 can be used to quantitatively evaluate the rate of photodecomposition. The kinetics of photodecomposition of organics on TiO_2 has been explained in terms of a Langmuir model.[13,15−17] At a low concentration of substrate (i.e., the molecule to be decomposed) this model predicts simple pseudo-first-order kinetics with respect to the substrate concentration. When the data in Figure 5 are plotted accrding to this model, straight-line plots were obtained and the decomposition rate constant can be calculated from the slope. The fibrillar catalyst shows a rate constant of 0.03 min^{-1}, as opposed to a rate constant of 0.003 min^{-1} for the thin-film catalyst.

ZnO and WO_3 Fibrils. Figure 6 shows SEM images of solid ZnO fibrils obtained within the pores of the 200 nm diameter alumina template membranes. The surface layer is not completely removed which makes the fibers stick together. As was the case for TiO_2, these fibrils are 200 nm in diameter and 50 μm long. These solid fibrils were obtained using a sol at 20 °C

and an immersion time of 1 min. By analogy to the TiO_2 case, hollow ZnO tubules are obtained if lower temperatures and shorter immersion times are used. An absorption spectrum for a composite membrane containing these ZnO fibrils is shown in Figure 7. Again, the bandgap absorption for ZnO is observed.[10,18] Finally, when exposed to 366 nm light, these fibrils showed the characteristic[10] greenish-yellow bulk luminescence of ZnO.

Figure 8 shows SEM images of solid WO_3 fibrils obtained within the pores of the 200 nm diameter alumina template membrane. As was the case for the other materials, these fibrils are 200 nm in diameter and 50 μm long. The SEM picture shows that some of the surface layer is not removed as in the case of ZnO. These solid fibrils were obtained using an immersion time of 1 min and temperature of 20 °C. We are especially interested in exploring the electrochemistry of these WO_3 fibrils, to obtain the corresponding tungsten bronzes.

Conclusions

We have shown that sol−gel synthetic methods can be used with the template-based approach for preparing nanomaterials to yield semiconductor nanostructures. This marriage of sol−gel and template methods should be applicable to a large number of materials. Both fibrillar and tubular nanostructures are possible, and single-crystalline nanostructures of the metastable anatase phase can be obtained. We are currently exploring applications of these nanostructures in photocatalysis, electrochemistry, battery research and development, photoelectrochemistry, and enzyme immobilization.

Acknowledgment. Financial support for this work was provided by the U.S. Department of Energy (DE-FG03-95ER14576) and by the National Science Foundation (CTS-9423090).

CM9605577